AJCS

Aust J Crop Sci. 19(11):1090-1099 (2025) | https://doi.org/10.21475/ajcs.25.19.11.p15

ISSN:1835-2707

Silicon nanoparticles for the control of Fusarium sp. in maize

Severino de Carvalho Neto*, Clint Wayne Araújo da Silva, Helder Windson Gomes dos Santos Oliveira, Lucy Gleide da Silva, Mirelly Coêlho de Souza, Ana Cecília da Rocha Oliveira, Severino Moreira d Silva, Adjair José da Silva, Edcarlos Camilo da Silva, Hilderlande Florêncio da Silva, Luciana Cordeiro do Nascimento

Universidade Federal da Paraíba (UFPB)- Centro de Ciências Agrárias (CCA) - 12 Rodovia, PB-079, 58397-000- Areia - PB, Brasil

*Corresponding author: neto.agronomia97@gmail.com

Submitted: 16/04/2025

Revised: 17/06/2025

Accepted: 21/08/2025

Abstract: Maize is one of the most important crops worldwide but is highly susceptible to fungal diseases, particularly those caused by Fusarium sp., which compromise grain yield and quality. Conventional control relies on fungicides, posing risks of pathogen resistance and environmental impacts. Although silicon is not essential for plants, it can induce resistance, making it a promising sustainable alternative. This study evaluated the use of silicon nanoparticles for the control of Fusarium sp. both in vitro and in maize plants. The experiment was conducted at the Phytopathology Laboratory of the Federal University of Paraíba (UFPB), Campus II, Areia - PB, testing silicon nanoparticle concentrations (0 to 5 g/L) and a commercial fungicide (Prothioconazole + Trifloxystrobin). In the in vitro assay, mycelial growth and sporulation of the fungus were analyzed, while in the in vivo test, and at 30 days after sowing (DAS), the Jabatão variety was inoculated, and growth, biomass, chlorophyll content, chlorophyll fluorescence, and pathogen infection rate were evaluated. The in vitro results indicated that doses of 1 to 3 g/L reduced mycelial growth, whereas sporulation was more inhibited at 4 g/L. In the in vivo test, infection was eliminated at 1 g/L, with no significant effects on physiological or biometric variables. Multivariate analysis identified shoot length, shoot dry mass, and root volume as key predictors of infection. These findings suggest that silicon has potential for Fusarium sp. control, warranting further studies to elucidate its mechanisms and optimize its application.

Keywords: Alternative control; fusarium wilt; infection rate; mycelial growth; plant physiology.

Abbreviations: B.O.D. (Biochemical Oxygen Demand); BD (Basal Diameter); CAS (Center for Agricultural Sciences); CD (Colony Diameter); DAS (Days After Sowing); F_m (Maximum Fluorescence); F0 (Initial Fluorescence); F_v (Variable Fluorescence); F_v/F_m (Quantum Yield of Photosystem II); F_v/F_0 (Fluorescence Ratio); FCI a (Falker Chlorophyll Index a); FCI a/b (Falker Chlorophyll Index a/b Ratio); FCI b (Falker Chlorophyll Index b); FCI T (Falker Chlorophyll Index Total); FUOP (Federal University of Paraíba); IR (Infection Rate); MGIP (Mycelial Growth Inhibition Percentage); MGSI (Mycelial Growth Speed Index); NL (Number of Leaves); PAL (Phenylalanine Ammonia-Lyase); PCA (Principal Component Analysis); PDA (Potato Dextrose Agar); PHYLA (Phytopathology Laboratory); POX (Peroxidase); PPO (Polyphenol Oxidase); RDM (Root Dry Mass); RV (Root Volume); SDM (Shoot Dry Mass); SDW (Sterile Distilled Water); SIP (Sporulation Inhibition Percentage); SL (Shoot Length); SP (Spore Production).

Introduction

Maize (*Zea mays* L.) is a globally significant crop due to its adaptability to dryland conditions and its role as a staple food in many regions (García-Lara & Serna-Saldívar, 2019). It is also widely used as animal feed (Sots and Bnyiak, 2018). As the world's most important cereal, maize has an annual production exceeding 1 billion tons and plays a crucial role in global food and energy security, being a high-yielding and export-oriented crop (Wang & Hu, 2021).

Despite its high productivity, maize is highly susceptible to a broad range of diseases, which can reduce yields and affect grain quality (Liliane and Charles, 2020). Among these, *Fusarium* spp. are particularly significant as major fungal pathogens affecting various crops worldwide, including maize, where they cause ear rot. These fungi persist in crop residues and infect plants through root wounds, colonizing xylem vessels and spreading systemically (Solórzano-Solórzano et al., 2024). The infection leads to symptoms such as wilting, root and stem rot, foliar lesions, and the death of both young and mature plants (Punja & Roberts, 2021).

Fusarium infection can occur both pre- and post-harvest, with severity influenced by specific environmental conditions, particularly high temperature and humidity (Al-Husnan et al., 2020; García-Díaz et al., 2020). Additionally, chemical control using fungicides significantly increases production costs (Arias-Martín et al., 2021; Solórzano-Solórzano et al., 2024).

Furthermore, mycotoxin contamination leads to economic losses in the food processing industry due to the need to discard contaminated grains.

The primary strategy for *Fusarium* control in maize relies on synthetic fungicides. However, their excessive use can result in pathogen resistance and negative environmental impacts, such as soil and water pollution, which ultimately affect local biodiversity (Seepe et al., 2021).

Although silicon is not classified as an essential nutrient for plants, it plays a crucial role in enhancing plant defense mechanisms (Yang et al., 2022). Silicon strengthens cell walls, increasing physical resistance against pathogens and pests (Verma et al., 2021). Moreover, it induces systemic resistance by activating biochemical and molecular processes that improve plant responses to biotic stresses, including fungal and bacterial infections as well as insect attacks (Islam et al., 2021). Silicon also mitigates biotic stress by enhancing antioxidant enzyme activity, promoting antimicrobial compound production, and regulating the expression of defense-related genes (Singh et al., 2020; Yu et al., 2022; Zhang et al., 2023). As a sustainable alternative for disease control, silicon reduces disease severity and enhances plant resistance (Verma et al., 2021).

Nanosilicon has emerged as a promising alternative to conventional silicon, primarily due to its properties that significantly enhance its effectiveness in plant protection (Gancarz et al., 2023). Owing to their dimensions of less than 100 nanometers, silicon nanoparticles are more readily absorbed by plant tissues, promoting more efficient distribution and activation of physiological defense mechanisms. This facilitates a more effective induction of resistance responses and the formation of physical barriers against pathogens (Elangovan et al., 2021; Ma, 2004). Furthermore, their high reactivity and increased specific surface area enable more intense interactions with cellular structures and biochemical compounds within the plant, thereby enhancing their beneficial effects (Gancarz et al., 2023).

Given this context, this study aimed to evaluate the efficacy of different doses of silicon nanoparticles in controlling *Fusarium* sp. in maize plants.

Results and discussion

According to the analysis of variance results (Table 1), a significant effect was observed for the variables studied in the *in vitro* experiment. However, no significant effect was found on the physiological variables in the *in vivo* experiment or on enzymatic activity, except for the infection rate (IR).

For the variables CD, MGSI, and MGIP the 1, 2, and 3 g/L doses of silicon nanoparticles showed better results than the control (0 g/L). Figures 1A, 1B, and 1C indicate that these doses negatively affect fungal development, suggesting that silicon nanoparticles interfere with mycelial growth. This effect may be due to alterations in nutrient availability or direct impacts on the fungal cell wall (Van Bockhaven et al., 2013; Coskun et al., 2019).

Similar results were reported by Sun et al. (2022), who evaluated the inhibitory potential of silicon on *Fusarium oxysporum* f. sp. *cucumerinum* mycelial growth in BDA medium. As in the present study, intermediate silicon doses yielded the most promising outcomes, though the observed effects were less pronounced. In *F. oxysporum*, mycelial growth inhibition reached 23% at a 3 mmol/L silicon dose, whereas in the present study, inhibition was only 5.0% at 3 g/L of silicon nanoparticles. This result was statistically similar to the 1 g/L dose, which inhibited growth by 3.5% (Figure 1C).

Regarding spore production (Figure 1D), silicon nanoparticle treatments (1, 2, 4, and 5 g/L) effectively reduced fungal reproductive capacity. These findings are crucial for disease management, as symptom severity and pathogen dissemination depend on inoculum quantity. However, the 3 g/L treatment did not significantly differ from the control (0 g/L). All tested doses reduced sporulation inhibition percentage (SIP) relative to the untreated control, negatively affecting spore production.

The application of silicon nanoparticles significantly influenced the *Fusarium sp.* infection rate (IR) in maize plants (Figure 2), but no significant effects were observed on the evaluated biometric, physiological, or enzymatic variables.

For IR reduction, the 1 g/L silicon dose yielded the best results, completely inhibiting pathogen development compared to the control treatment, which had a 58% IR. This effect was statistically similar to that of the fungicide-based treatment. The 2 and 4 g/L doses reduced IR by 71% relative to the control. In contrast, the 3 and 5 g/L doses resulted in only 43% and 29% reductions, respectively (Table 2).

The reduction in IR following silicon application may be attributed to increased production of fungitoxic metabolites and phenolic compounds, which play a role in plant defense (Whan et al., 2016). These findings suggest that silicon may function as a potential infection control agent, supporting previous studies that highlight its role in inducing plant defense mechanisms (Pozza et al., 2015; Verma et al., 2021). Additionally, silicon may induce cellular modifications that hinder fungal penetration and development, such as the deposition of dense materials in endodermal and vascular cells (Nachaat, 2024).

Regarding plant growth, variables such as shoot length, basal diameter, number of leaves, and root volume showed no significant response to silicon nanoparticle doses. These findings align with those of Coskun et al. (2019) and Debona et al. (2020), who reported that silicon does not always induce visible changes in plant growth, particularly under conditions without significant biotic or abiotic stress. Similar results were observed by Porcino et al. (2024). The lack of effects on growth may be attributed to the relatively short evaluation period or the nutrient availability in the substrate, which could have masked potential responses to silicon application (Etesami & Jeong, 2021). Additionally, silicon primarily enhances plant defense mechanisms and structural reinforcement, which do not always translate into immediate biometric changes (Vivancos et al., 2015; Verma et al., 2021).

The physiological parameters evaluated, including chlorophyll indices (CI a, CI b, total CI, and CI a/b) and fluorescence variables (F0, Fm, Fv/Fm, Fv/F0), were also unaffected by silicon treatments. The influence of silicon on photosynthetic

Table 1. Summary of analysis of variance for colony diameter (CD), mycelial growth speed index (MGSI), mycelial growth inhibition percentage (MGIP), spore production (SP), sporulation inhibition percentage (SIP), shoot length (SL), basal diameter (BD), number of leaves (NL), root volume (RV), variable fluorescence (Fv), initial fluorescence (F0), maximum fluorescence (Fm), quantum yield of photosystem II (Fv/Fm), fluorescence ratio (Fv/F0), shoot dry mass (SDM), root dry mass (RDM), Falker chlorophyll index a (FCI a), b (FCI b), total (FCI T), and a/b ratio (FCI a/b), infection rate (IR), and enzyme activity of peroxidase (POX), polyphenol oxidase (PPO), and phenylalanine ammonia-lyase (PAL), as a function of different silicon concentrations.

Sources of variation		DF	Mean squares					
			CD	MGSI	MGIP	SP	SIP	
Treatments		6	111.1150**	10.6426**	13717.8721**	125946.6224**	5181.0941**	
Concentrations		5	0.4832**	0.0741**	59.6596**	34788.9109**	1003.7483**	
Concentrations additional	VS.	1	664.2744**	63.4848**	82008.9344**	581735.1802**	26067.8233*	
Residual		63	0.1405	0.0034	17.3516	6921.1337	20.8979**	
CV (%)			4.96	2.52	25.78	26.34	13.78	
			SL	BD	NL	RV	Fv	
Block		3	48.0108 ns	5.3756**	0.1796 ns	807.2436*	0.0085260*	
Treatments		6	$108.9299\mathrm{ns}$	$0.5502\mathrm{ns}$	$0.0634\mathrm{ns}$	55.0588 ns	0.0004887 ns	
Concentrations		5	29.2112 ns	$0.4190\mathrm{ns}$	$0.0379\mathrm{ns}$	62.6850 ns	0.0004115 ns	
Concentrations additional	vs.	1	507.5238*	1.2065 ns	0.1911 ns	16.9278 ns	0.0008747 ns	
Residual		18	77.6482	0.6090	0.0810	165.4223	0.0021601	
CV (%)			9.62	6.71	9.33	21.98	6.56	
			Fo	Fm	Fv/Fm	Fv/Fo	SDM	
Block		3	387.5807 ns	12239.2421 ns	7.3653 ns	4.4215 ns	19.1771 ns	
Treatments		6	1003.7857 ns	9363.30026 ns	2.5783 ns	4.6518 ns	11.8473 ns	
Concentrations		5	1059.8185 ns	11083.9519 ns	3.0935 ns	5.5587 ns	11.1409 ns	
Concentrations additional	vs.	1	723.6216 ns	760.0423 ns	2.7573 ns	1.1684 ns	15.3797 ns	
Residual		18	1005.2690	12455.2297	2.3217	4.0139	7.6420	
CV (%)			21.81	21.71	31.26	36.34	15.18	
			RDM	FCI a	FCI b	FCI T	FCI a/b	
Block		3	74.0253**	4.3060 ns	0.1514 ns	5.5793 ns	0.379087 ns	
Treatments		6	$10.2760\mathrm{ns}$	$1.1173\mathrm{ns}$	$0.0166\mathrm{ns}$	1.3979 ns	0.009081 ns	
Concentrations		5	10.4245 ns	$0.8567\mathrm{ns}$	$0.0155\mathrm{ns}$	1.0961 ns	0.003739 ns	
Concentrations additional	vs.	1	9.5338 ns	2.4208 ns	$0.0222\mathrm{ns}$	2.9072 ns	0.035790 ns	
Residual		18	13.0883	2.9164	0.1510	4.3294	0.129329	
CV (%)			24.45	7.35	11.85	7.85	5.03	
			IR	POX	PPO	PAL		
Block		3	1.8460 ns	3475.4893 ns	0.1443 ns	0.0947 ns		
Treatments		6	26.7983**	1634.0953 ns	0.2480 ns	0.1880 ns		
Concentrations		5	22.1129**	1247.1093 ns	$0.2397\mathrm{ns}$	0.2116 ns		
Concentrations additional	vs.	1	50.2257**	3569.0252 ns	0.2893 ns	$0.0702\mathrm{ns}$		
Residual		18	0.8482	1762.4751	0.2485	0.2098		
CV (%)			21.51	30.08	26.80	31.01		

ns, * and ** - Not significant and significant at $p \le 0.05$ and $p \le 0.01$ by F test, respectively; CV - Coefficient of variation; DF - Degrees of freedom

efficiency and chlorophyll metabolism has been extensively studied, with reports suggesting that its effects depend on the level of stress experienced by the plants (Liang et al., 2007). Thus, the absence of differences between treatments suggests that the experimental conditions did not induce sufficient stress for silicon to exert a significant physiological effect. Enzymatic activity analysis of peroxidase (POX), polyphenol oxidase (PPO), and phenylalanine ammonia-lyase (PAL) also revealed no significant differences among treatments. These enzymes play a crucial role in plant defense against pathogens, being involved in phenolic compound synthesis and cell wall lignification (Van Bockhaven et al., 2013). Silicon application

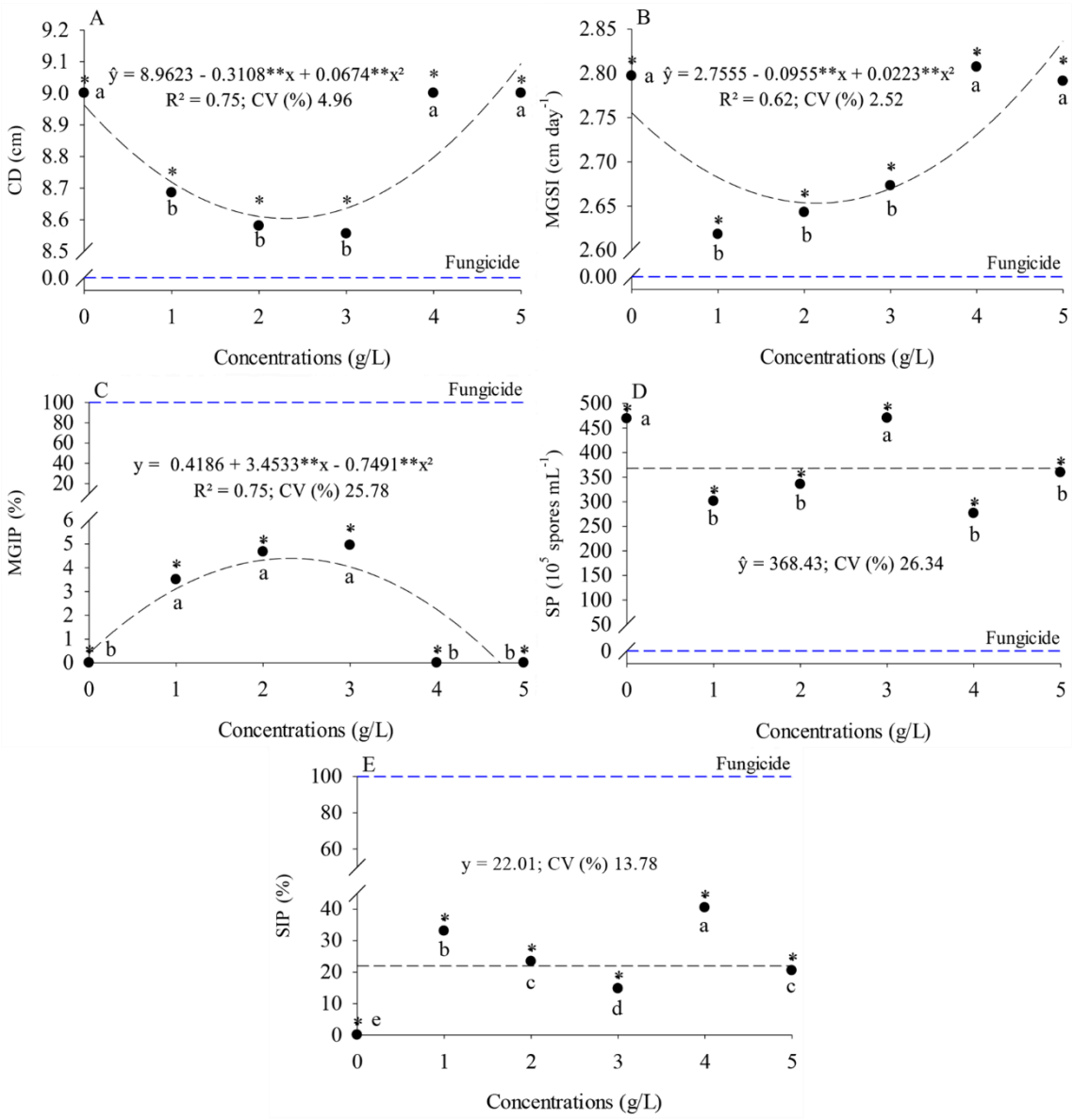


Fig 1. Colony diameter (CD), mycelial growth speed index (MGSI), mycelial growth inhibition percentage (MGIP), spore production (SP), and sporulation inhibition percentage (SIP) of *Fusarium* sp. exposed to different silicon concentrations. Means followed by the same letter do not differ from each other according to the Scott-Knott test ($p \le 0.05$), and means followed by * differ significantly from the fungicide treatment according to Dunnett's test at a 5% probability level.

can enhance their activity in pathogen-infected plants; however, this response varies depending on plant species, pathogen type, and environmental conditions (Rémus-Borel et al., 2005; Vivancos et al., 2015). In this study, the lack of enzymatic response may be related to the pathogen exposure period or the silicon concentration used.

Moreover, plant defense activation peaks may occur shortly after pathogen inoculation and could be dose-dependent (Cherif & Bélanger, 1994). This dynamic may have hindered the detection of significant differences in enzyme activity among treatments. Although the plants were treated and inoculated, tissue samples were collected from leaves only 30 days after sowing and inoculation, possibly missing the optimal window for detecting defense-related enzyme activation.

Porcino et al. (2023) also observed no increase in POX, PPO, or PAL activity in melon plants (*Cucumis melo*) treated with different silicon sources via foliar application, with treatments showing no differences from each other or from the negative control. Similarly, Whan et al. (2016) demonstrated that the defense mechanisms of cotton plants (*Gossypium hirsutum*) supplied with silicon were activated more rapidly and intensely upon inoculation, supporting the hypothesis that pathogen presence is required to trigger and regulate silicon-induced defense responses.

Although silicon did not induce changes in biometric, physiological, or enzymatic parameters—unlike the findings of Sun et al. (2022)—its ability to reduce *Fusarium sp.* infection reinforces its potential as a phytosanitary management strategy. Future studies should assess its efficacy under different environmental conditions, concentrations, and application methods, as well as explore its effects at more advanced crop development stages and clarify the mechanisms involved in disease suppression (Ma; Yamaji, 2006; Verma et al., 2021).

Principal component analysis (PCA) indicated that two components were necessary to adequately explain variability among treatments. Principal components PC1 and PC2 accounted for 45.5% and 21.8% of the total variance, respectively, representing a cumulative variance of 67.3% for the evaluated characteristics (Table 2).

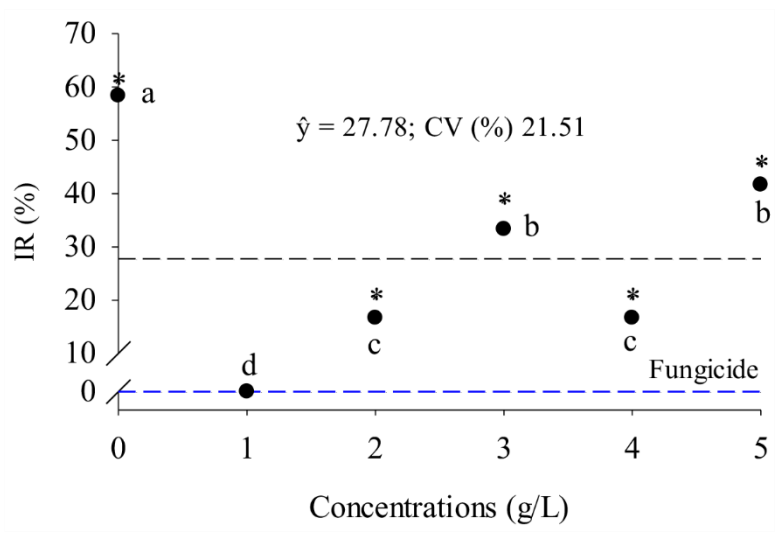


Fig 2. Infection rate (IR) of *Fusarium* sp. in maize plants (*Zea mays* L.) originating from inoculated seeds treated with different silicon concentrations. Means followed by the same letter do not differ from each other according to the Scott-Knott test ($p \le 0.05$), and means followed by * differ significantly from the fungicide treatment according to Dunnett's test at a 5% probability level.

Table 2. Contribution of the variables to each axis of the principal components in the physiological variables of maize plants

(Zea mays L_.) from seeds inoculated with Fusarium sp. and treated with silicon concentrations.

Wastalla	Autovectors			
Variables	CPA ₁	CPA ₂		
Shoot length (SL)	0.338	-0.092		
Basal diameter (BD)	0.180	0.379		
Number of leaves (NL)	0.250	0.033		
Root volume (RV)	0.210	0.392		
Shoot dry mass (SDM)	0.311	0.226		
Root dry mass (RDM)	0.181	0.242		
Chlorophyll a (FCI a)	-0.320	0.250		
Chlorophyll b (FCI b)	-0.318	0.224		
Total chlorophyll (FCI T)	-0.321	0.246		
Chlorophyll a/b ratio (FCI a/b)	-0.175	0.228		
Quantum yield of photosystem II (F_v/F_m)	0.312	-0.162		
Fv/F0 ratio	0.214	-0.082		
Peroxidase (POX)	0.176	-0.223		
Polyphenol oxidase (PPO)	-0.258	-0.140		
Phenylalanine ammonia-lyase (PAL)	-0.127	-0.382		
Infection rate (IR)	-0.152	-0.330		
Autovalues	7.283	3.495		
Cumulative variance (%)	45.5	21.8		

The most representative variables in PC1 were shoot length (SL), shoot dry mass (SDM), chlorophyll a (CI a), chlorophyll b (CI b), total chlorophyll (CI T), and quantum yield of photosystem II (Fv/Fm). In PC2, the most relevant variables were basal diameter (BD), root volume (RV), phenylalanine ammonia-lyase (PAL), and infection rate (IR).

Principal component and cluster analyses revealed the formation of four distinct groups (Figures 3A and 3B). In the first group (Dose 0), higher activity of polyphenol oxidase (PPO) and phenylalanine ammonia-lyase (PAL) was observed; however, the infection rate (IR) was the highest among all groups (Figure 3B). In the second group (Dose 1), chlorophyll a (CI a), chlorophyll b (CI b), and total chlorophyll (CI T) exhibited better performance (Figure 1A). However, root volume (RV), basal diameter (BD), the chlorophyll a/b ratio (CI a/b), and PPO activity were also influenced by the treatment, as was the infection rate (Figure 3B).

The fourth group (Fungicide) presented the highest values for basal diameter (BD), quantum yield of photosystem II (Fv/Fm), shoot dry mass (SDM), shoot length (SL), number of leaves (NL), and peroxidase (POX) activity (Figure 3A). However, Figure 3B shows that this treatment significantly reduced chlorophyll indices.

Regarding the third group (Doses 2, 3, 4, and 5), the treatments followed a similar pattern, standing out in root volume (RV), quantum yield of photosystem II (Fv/Fm), Fv/F0 ratio, shoot dry mass (SDM), and the chlorophyll a/b ratio (CI a/b) (Figure

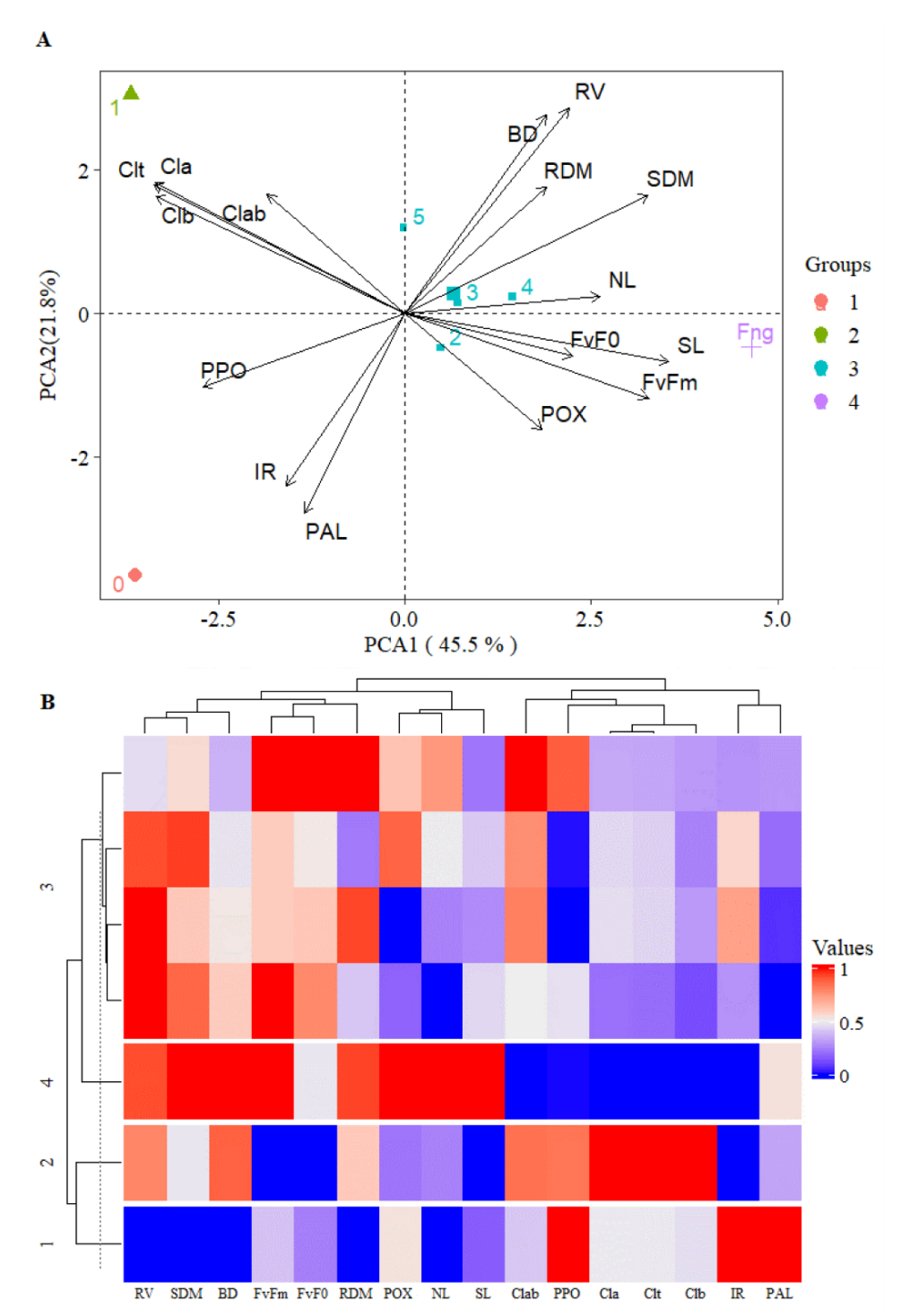


Fig 3. Principal component analysis (PCA) (A) and heatmap (B) of the physiological variables of maize plants (*Zea mays* L.) originating from seeds inoculated with *Fusarium* sp. and treated with silicon concentrations. Shoot length (SL), basal diameter (BD), number of leaves (NL), root volume (RV), quantum yield of photosystem II (Fv/Fm), fluorescence ratio (Fv/F0), shoot dry mass (SDM), root dry mass (RDM), Falker chlorophyll index *a* (CI *a*), b (CI *b*), total (CI *T*), and a/b ratio (CI *ab*), infection rate (IR), and the activity of the enzymes peroxidase (POD), polyphenol oxidase (PPO), and phenylalanine ammonia-lyase (PAL).

3B). This group exhibited lower variability, with more contained dispersion and less individual impact on the main variables.

Regression tree analysis for infection rate (IR) prediction identified the variables with the greatest influence on IR (Figure 4). Shoot length (SL), shoot dry mass (SDM), and root volume (RV) had the highest impact on IR, with relative importance values of 19%, 15%, and 13%, respectively. Thus, plants with SDM values of \leq 16 g, SL <87 cm, and RV \leq 67 cm³ were more susceptible to higher infection rates by *Fusarium sp.*. Consequently, plants with these characteristics may face difficulties in nutrient and water uptake, which directly affects their ability to resist infections.

The results of the regression tree analysis support the idea that specific morphophysiological traits are correlated with plant susceptibility to *Fusarium sp.*, reinforcing the importance of these variables in disease monitoring and management.

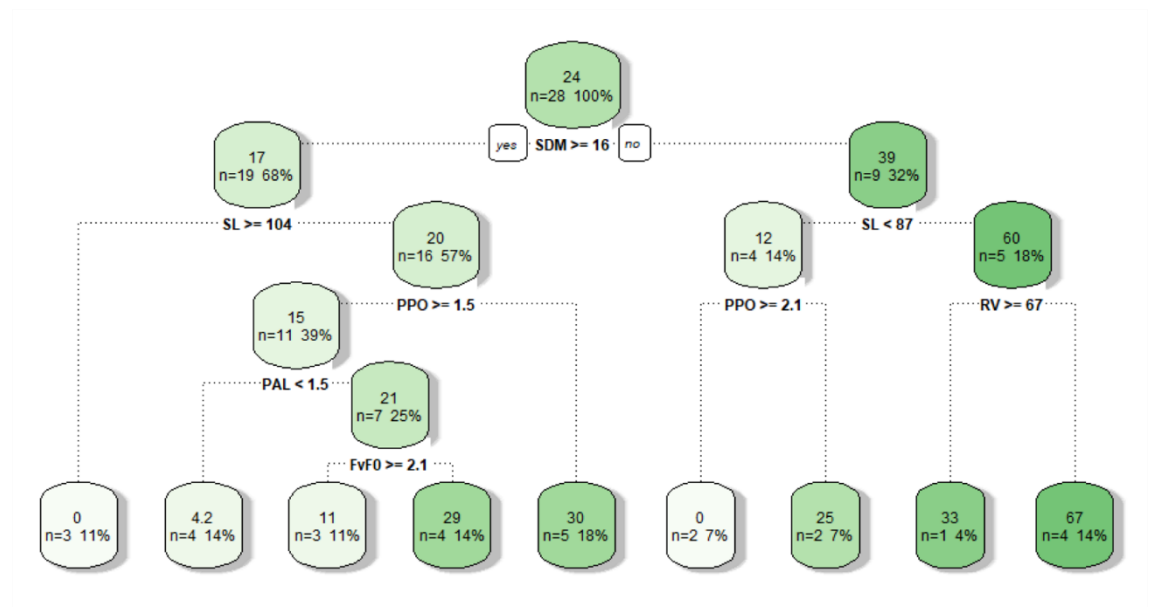


Fig 4. Graphical representation of the regression tree for predicting the infection rate (IR) based on the variables shoot dry mass (SDM), shoot length (SL), polyphenol oxidase (PPO), phenylalanine ammonia-lyase (PAL), root volume (RV), and the (Fv/F0) ratio.

Materials and methods

Experimental location

The experiment was conducted at the Phytopathology Laboratory (PHYLA) and in a greenhouse, both affiliated with the Department of Crop Science and Environmental Sciences at the Center for Agricultural Sciences (CAS) of the Federal University of Paraíba (FUOP), Campus II, Areia, Paraíba.

Isolation of Fusarium sp. and acquisition of traditional maize seeds

The *Fusarium* sp. isolate was obtained from maize plants exhibiting characteristic symptoms of vascular discoloration, wilting, root rot, and plant desiccation, collected in the region of Areia, PB.

Symptomatic plants were collected, and tissue fragments were excised from the boundary between the healthy and infected areas using a scalpel. The fragments were then surface-sterilized by immersion in 70% ethanol for 30 seconds, followed by 1% sodium hypochlorite for 2 minutes, and rinsed three times with sterile distilled water (SDW) for 1 minute. The fragments were then dried on sterile filter paper. Under aseptic conditions, the tissue fragments were transferred to 9 cm diameter Petri dishes containing potato dextrose agar (PDA).

The plates were incubated in a *Biochemical Oxygen Demand* (B.O.D.) chamber at $25 \pm 2^{\circ}$ C under a 12-hour photoperiod for seven days. The isolate was subcultured on PDA until a pure culture was obtained and subsequently preserved using the Castellani (1939) method. For the experiments, the isolate was maintained in a B.O.D. chamber at $25 \pm 2^{\circ}$ C with a 12-hour photoperiod for seven days.

Traditional maize seeds were obtained from subsistence farmers in Montadas, PB, from the 2024 harvest. Initially, the seeds were disinfected in a 1% sodium hypochlorite solution for three minutes, followed by two rinses with SDW. The seeds were then immersed in 100 mL of SDW containing the respective treatments for five minutes.

The treatments applied were as follows: (T1) – Prothioconazole + Trifloxystrobin (Fungicide) (166.6 μ L/100 mL) (Fungicide); (T2) - Control (ADE); and nano-silicon doses: (T3) – 1 g L⁻¹; (T4) – 2 g L⁻¹; (T5) – 3 g L⁻¹; (T6) – 4 g L⁻¹; and (T7) – 5 g L⁻¹; diluted in SDW.

In vitro assay

The *in vitro* assay was conducted by distributing 10 mL of PDA medium supplemented with different concentrations of nano-silicon into 9 cm diameter Petri dishes. A 5 mm diameter disk from a pure *Fusarium* sp. colony was placed at the center of each plate. The plates were incubated in a B.O.D. chamber at $25 \pm 2^{\circ}$ C under a 12-hour photoperiod. Colony diameter measurements were taken every 24 hours for seven days using a graduated ruler. Measurements were recorded in two perpendicular directions across the colony edges, and the average was calculated.

Spore counting was performed on the seventh day by adding 10 mL of sterile distilled water (SDW) to the Petri plates to release the spores using a soft-bristle brush. The spore suspension was filtered through a double layer of sterile gauze and quantified using a Neubauer chamber.

In vivo assay

Before treatment application, maize seeds were disinfected by immersion in a 1% sodium hypochlorite solution for three minutes, followed by two rinses with SDW. The seeds were then dried on paper towels at $25 \pm 2^{\circ}$ C, treated as previously described for five minutes, and placed on Petri plates containing a double layer of sterile filter paper.

After 24 hours, seeds were inoculated with *Fusarium* sp. using the suspension method. This was achieved by adding 10 mL of SDW to a Petri plate to release spores with a soft-bristle brush, followed by filtration through a double layer of sterile gauze. Spore quantification was performed using a hemocytometer, and the suspension was adjusted to 1×10^5 spores mL⁻¹. The seeds were immersed in the suspension for five minutes before sowing.

Greenhouse sowing was carried out in 30×15 cm plastic pots filled with sterilized Mecplant® commercial substrate. Three seeds were sown per pot, and on the 15th day, thinning was performed, leaving the most vigorous plant. Plants were irrigated manually daily, and at 30 days after sowing (DAS), plant height (from the stem base to the apex) and leaf number were recorded using a graduated ruler.

At the end of the evaluations, the infection rate (IR) was assessed using stem base fragments. Sections (0.5 mm) were excised with a sterile scalpel, surface-sterilized in 70% ethanol for 30 seconds, followed by 1% sodium hypochlorite for three minutes, and rinsed twice with SDW. The fragments were transferred to 9 cm Petri dishes containing PDA and incubated for eight days in a B.O.D. chamber at $25 \pm 2^{\circ}$ C under a 12-hour photoperiod.

Pathogen etiology was confirmed using an optical microscope by examining vegetative and reproductive structures and comparing them to descriptions provided by Seifert et al. (2011).

Root volume was determined by immersing the roots in a graduated cylinder containing 800 mL of water. Shoot dry mass (SDM) was measured by placing samples in Kraft paper bags and drying them in an oven at 65°C until reaching a constant weight (72 hours).

Chlorophyll indices (chlorophyll a, b, and total) were determined using a non-destructive method with a portable chlorophyll meter (ClorofiLOG®, model CFL 1030, Porto Alegre, RS), expressed as the Falker Chlorophyll Index (FCI). Fluorescence variables were analyzed using a modulated fluorometer (Sciences Inc., Model OS-30p, Hudson, USA). Leaves were dark-adapted for 30 minutes using leaf clips before fluorescence readings. The parameters measured included initial fluorescence (F_0), maximum fluorescence (F_m), variable fluorescence ($F_v = F_m - F_0$), the F_v/F_0 ratio, and the quantum yield of photosystem II (F_v/F_m).

Enzymatic Activity Assessment

The activity of peroxidase (POX), polyphenol oxidase (PPO), and phenylalanine ammonia-lyase (PAL) was evaluated and expressed in absorbance units per minute per milligram of protein (UA·min⁻¹·mg⁻¹ protein).

Enzymatic activity assays were conducted using protein extracts obtained from homogeneous samples of 1 g of the middle third of the first fully developed leaf from each plant in the *in vivo* assay. Samples were collected 30 days after sowing. For protein extraction, leaf samples were fragmented in liquid nitrogen and macerated in 0.1 M sodium acetate buffer (pH 5.0) under cold bath conditions. The extracts were then centrifuged at -4°C and 12,000 rpm for 15 min to obtain the supernatant containing soluble proteins.

Total protein content was quantified using the Bradford method (1976). The enzymatic assay methodologies followed the protocols described by Porcino et al. (2023).

Experimental design and statistical analysis

A completely randomized design with ten replicates was used for the in vitro assay, while a randomized block design with four replicates was adopted for the in vivo assay. Both experiments included seven treatments. Each experimental unit consisted of one Petri dish in the *in vitro* assay and three pots, each containing a single plant, in the *in vivo* assay. Statistical analysis was performed using R® software version 4.4.1 (R Core Team, 2024). Data were subjected to analysis of variance (ANOVA) and polynomial regression, testing linear and quadratic models. Means for each concentration were compared using the Scott-Knott test ($p \le 0.05$), while comparisons between individual treatments and the fungicide control were conducted using Dunnett's test at a 5% probability level. Infection rate (IR) values were transformed as ($\sqrt{x} + 1$) according to Bartlett (1947) prior to analysis.

Principal Component Analysis (PCA) was performed to reduce data dimensionality, followed by hierarchical clustering using Ward's method, with clustering set to four groups. Variable selection was based on an eigenvector criterion, considering a threshold of 0.7 divided by the square root of the variance for each dimension, allowing the identification of the most significant variables in dimensions 1, 2, and 3. A PCA biplot was used to visualize the identified clusters and the two principal components (PC1 and PC2), which explained the highest percentage of variance.

The heatmap was generated following data normalization and the creation of an interactive graph. Initially, data were converted into a matrix, with columns normalized to a 0–1 scale to ensure uniform variable scaling. For regression tree analysis, a model was fitted to predict IR based on other dataset variables. The regression tree was constructed using the ANOVA method, suitable for continuous response variables.

Conclusions

Silicon nanoparticle concentrations of 1, 2, and 3 g/L were effective in reducing the infection rate of *Fusarium sp.* in maize plants under *in vitro* fungal development. Nano-silicon did not influence morphological (shoot length, basal diameter, number of leaves, and root volume), physiological (chlorophyll and fluorescence indices), or enzymatic (peroxidase, polyphenol oxidase, and phenylalanine ammonia-lyase) variables. Principal component analysis (PCA) revealed the formation of distinct groups, highlighting the influence of silicon on different variables but without a clear pattern of improvement in physiological parameters. Additionally, regression tree analysis indicated that shoot length (SL), shoot dry mass (SDM), and root volume (RV) were the most relevant variables for predicting infection rates.

References

Al-Husnan L, Al-Kahtani M, Farag R (2020) Molecular characterization of fumonisin mycotoxin genes of Fusarium sp isolated from corn and rice grains. Sultan Qaboos Univ J Sci. 24(2):78.

Arias-Martín M, Haidukowski M, Farinós GP, Patiño B (2021) Role of Sesamia nonagrioides and Ostrinia nubilalis as vectors of Fusarium spp. and contribution of corn borer-resistant BT maize to mycotoxin reduction. Toxins. 13(11).

Bartlett MS (1947) The use of transformations. Biometrics. 3(1):39–52

Bradford MM (1976) A rapid and sensitive method for the quantitation of micrograms quantities for proteins utilizing the principle of protein-dye binding. Anal Biochem. 72:248–254

Castellani A (1939) Viability of some pathogenic fungi in distilled water

Chérif M, Asselin A, Bélanger RR (1994) Defense responses induced by soluble silicon in cucumber roots infected by Pythium spp. Phytopathology. 84:236–242

Coskun D, Deshmukh R, Sonah H, Menzies JG, Reynolds O, Ma JF, Bélanger RR (2019) The controversies of silicon's role in plant biology. New Phytol. 221(1):67–85.

Debona D, Rodrigues FA, Datnoff LE (2020) Silicon's role in plant stress reduction and why this element is still underutilized. I Plant Nutr. 43(7):948–965.

Elangovan H, Sengupta S, Narayanan R, Chattopadhyay K (2021) Silicon nanoparticles with UV range photoluminescence synthesized through cryomilling induced phase transformation and etching. J Mater Sci. 56(2):1515–1526.

Etesami H, Jeong BR (2021) Contribution of arbuscular mycorrhizal fungi, phosphate-solubilizing bacteria, and silicon to P uptake by plant: A review. Front Plant Sci. 12:699618.

Gancarz M, Umar A, Jabeen K, Ameen F, Iqbal S, Darwish D, Ahmad F (2023) Influence of silicon nano-particles on *Avena sativa* L. to alleviate the biotic stress of *Rhizoctonia solani*. Sci Rep. 13.

García-Díaz M, Gil-Serna J, Vázquez C, Botia MN, Patiño B (2020) A comprehensive study on the occurrence of mycotoxins and their producing fungi during the maize production cycle in Spain. Microorganisms. 8(1).

García-Lara S, Serna-Saldivar SO (2019) Corn history and culture. In: Corn. pp. 1-18

Islam W, Tayyab M, Khalil F, Hua Z, Huang Z, Chen H (2020) Defesa de plantas mediada por silício contra patógenos e pragas de insetos. Pest Biochem Physiol. 168:104641.

Liang Y, Sun W, Zhu YG, Christie P (2007) Mechanisms of silicon-mediated alleviation of abiotic stresses in higher plants: A review. Environ Pollut. 147(2):422–428.

Liliane TN, Charles MS (2020) Factors affecting yield of crops. In: IntechOpen.

Ma JF, Yamaji N (2006) Silicon uptake and accumulation in higher plants. Trends Plant Sci. 11(8):392-397.

Ma JF (2004) Role of silicon in enhancing the resistance of plants to biotic and abiotic stresses. Soil Sci Plant Nutr. 50(1):11–18

Nachaat S (2024) Silicon nonspecifically affects aggressiveness in head blight pathogens. J Agroaliment Process Technol.

Porcino MM, Oliveira VS, Silva EC, Nunes MS, Tico BM, Holanda GC, Souza MSS, Nascimento LC (2024) Field management of yellow melon (Cucumis melo L.) with silicon sources. Acta Sci Agron. 46:e68231

Porcino MM, Oliveira VS, Silva HF, Souza MS, Nascimento LC (2023) Essential oils in the management of Alternaria alternata f. sp. citri in 'Dancy' tangerine fruits. Rev Caatinga. 36(2):291–299

Pozza EA. Pozza AAE. Botelho DMS (2015) Silicon in plant disease control. Rev Ceres. 62(3):323-331

Punja ZK, Ni L, Roberts A (2021) The Fusarium solani species complex infecting cannabis (Cannabis sativa L., marijuana) plants and a first report of Fusarium (Cylindrocarpon) lichenicola causing root and crown rot. Can J Plant Pathol. 43(4):567–581.

R Core Team (2024) R: A language and environment for statistical computing. R Foundation for Statistical Computing. https://www.R-project.org/

Rémus-Borel W, Menzies JG, Bélanger RR (2005) Silicon induces antifungal compounds in powdery mildew-infected wheat. Physiol Mol Plant Pathol. 66(3):108–115

Seepe H, Nxumalo W, Amoo S (2021) Produtos naturais de plantas medicinais contra espécies de Fusarium fitopatogênicas: esforços de pesquisa atuais, desafios e perspectivas. Molecules. 26.

Seifert KA, Gams W (2011) The genera of Hyphomycetes-2011 update. Persoonia. 27(1):119-129

Singh A, Kumar A, Hartley S, Singh IK (2020) Silicon: Its ameliorative effect on plant defense against herbivory. J Exp Bot. 71(21):6730–6743.

Solórzano-Solórzano JA, Zambrano SMV, Olmedo JBV (2024) Fusarium spp. in corn crops: Identification, geographic distribution, symptoms, mycotoxins, disease cycle, control, and current and future challenges. Sci Agropecuaria. 15(4):537–556.

Sots SM, Bnyiak OV (2018) Use of corn grain in production of food products. Grain Prod Mix Fodder's. 18(2)

Sun S, Yang Z, Song Z, Wang N, Guo N, Niu J, Liu A, Bai B, Ahammed G, Chen S (2022) Silicon enhances plant resistance to Fusarium wilt by promoting antioxidant potential and photosynthetic capacity in cucumber (Cucumis sativus L.). Front Plant Sci. 13

Van Bockhaven J, De Vleesschauwer D, Höfte M (2013) Towards establishing broad-spectrum disease resistance in plants: Silicon leads the way. J Exp Bot. 64(5):1281–1293.

Verma KK, Song XP, Joshi A, Rajput VD, Singh M, Sharma A, Singh RK, Li DM, Arora J, Minkina T (2021) Recent trends in nano-fertilizers for sustainable agriculture under climate change for global food security. Nanomaterials. 11(2):259.

- Verma KK, Song XP, Tian DD, Guo DJ, Chen ZL, Zhong CS, Nikpay A, Singh M, Rajput VD, Singh RK, Minkina T, Li YR (2021) Influence of silicon on biocontrol strategies to manage biotic stress for crop protection, performance, and improvement. Plants. 10(10).
- Vivancos J, Labbé C, Menzies JG, Bélanger RR (2015) Silicon-mediated resistance of Arabidopsis against powdery mildew involves mechanisms other than the salicylic acid (SA)-dependent defence pathway. Mol Plant Pathol. 16(6):572–582.
- Wang J, Hu X (2021) Research on corn production efficiency and influencing factors of typical farms: Based on data from 12 corn-producing countries from 2012 to 2019. PLOS ONE. 16(7).
- Whan J, Dann E, Aitken E (2016) Effects of silicon treatment and inoculation with Fusarium oxysporum f. sp. vasinfectum on cellular defences in root tissues of two cotton cultivars. Ann Bot. 118(2):219–226.
- Yang J, Song J, Jeong BR (2022) Drenched silicon suppresses disease and insect pests in coffee plants grown in a controlled environment by improving physiology and upregulating defense genes. Int J Mol Sci. 23(7).
- Yu J, Yu X, Li C, Ayaz M, Abdulsalam S, Peng D, Qi R, Peng H, Kong L, Jia J, Huang W (2022) Silicon mediated plant immunity against nematodes: Summarizing the underline defence mechanisms in plant-nematode interaction. Int J Mol Sci. 23(22).
- Zhang Q, Wang J, Wang J, Liu M, Ma X, Bai Y, Chen Q, Sheng S, Wang F (2023) Nano-silicon triggers rapid transcriptomic reprogramming and biochemical defenses in Brassica napus challenged with Sclerotinia sclerotiorum. J Fungi. 9(11).